Single-molecule sandwich aptasensing on nanoarrays by Tethered Particle Motion analysis

Diana Soukarié[1], Philippe Rousseau[2], Maya Salhi[2a], Alexia de Caro[1], Jean-Marc Escudier[3], Catherine Tardin[1], Vincent Ecochard[1] and Laurence Salomé[1]*

[1] Institut de Pharmacologie et de Biologie Structurale, Université de Toulouse, CNRS, UPS, 31077 Toulouse, France

[2] Centre de Biologie Intégrative de Toulouse, Laboratoire de Microbiologie et Génétique Moléculaires, Université de Toulouse, CNRS, UPS, 31062 Toulouse, France

[3] Laboratoire de Synthèse et Physico-Chimie de Molécules d'Intérêt Biologique, Université de Toulouse, CNRS, UPS, 31062 Toulouse, France

[a]present address: Toulouse White Biotechnology, Campus de l'INSA, 31077 Toulouse, France

* Corresponding author:
Laurence Salomé laurence.salome@ipbs.fr +33 6 81 69 98 85
Institut de Pharmacologie et Biologie Structurale
205, route de Narbonne BP 64182, 31077 TOULOUSE cedex 4, FRANCE

Abstract

High-throughput single-molecule techniques are expected to challenge the demand of rapid, simple and sensitive detection methods in the health and environmental fields. Based on a single-DNA molecule biochip for the parallelization of Tethered Particle Motion analyses by videomicroscopy coupled to image analysis and its smart combination with aptamers, we successfully developed an aptasensor enabling the detection of single target molecules by a sandwich assay. One aptamer is grafted to the nanoparticles tethered to the surface by a long DNA molecule bearing the second aptamer in its middle. The detection and quantification of the target is direct. The recognition of the target by the pair of aptamers leads to a looped configuration of the DNA-particle complex associated to a restricted motion of the particles, which is monitored in real-time. An analytical range extending over three decades of target concentration with a limit of detection in the picomolar range was obtained for thrombin.

Keywords

TPM ; aptamer ; thrombin ; nanobiosensor ; DNA internal modification.

Development of rapid, simple and sensitive methods for the detection of substances in an aqueous medium is currently a field of technological research of intense activity. This research is driven by the need to detect ever-lower concentrations, at the source and without the need for complex instrumentation. Such objectives are shared by health and environmental applications. The identification and quantification of biomarkers in physiological fluids are needed to establish firmly a diagnostic or to monitor a disease evolution. Sensing technologies, integrated in point-of-care devices, for rapid and reliable measurements of low levels of biomarkers are highly demanded in the context of the development of personalized medicine [1]. A similar situation is found in the environmental field with the emerging issue of the presence of micropollutants in water. Those substances are found and can be harmful at very low concentrations urging for the development of novel methods for water quality monitoring [2, 3].

The efforts have led to a plethora of either novel or optimized existing sensing solutions with improved performances interesting both the clinical [4, 5] and water quality fields [6, 7]. Impressive advances, with in some cases sub-picomolar limit of detection (LOD), have been made mainly thanks to the introduction of nanotechnology through the use of nanomaterials or measurements at the nanometer scale [8].

For instance, nanoparticles, but even micron-sized beads, are the frequent support of single-molecule assays, which bear promising perspectives for the future of the sensing field. Making possible to detect single molecules and perform molecular counting, single-molecules methods recently popularized under the name of digital methods have the potential for reaching ultra-low detection limits [9, 10]. Developed at large scale using arrays, high-throughput single-molecule assays are good candidates for the next generation of analytical sensors. As proof, let us cite the work of Rissin *et al* [11] who developed single-molecule enzyme-linked immunosorbent assays on arrays of femtoliter-sized wells named SiMoA that accommodate individual beads with single immunocomplexes. This digital ELISA method detects proteins with a great increase in sensitivity compared to bulk conventional measurements, limits of detection lower than femtomolar are obtained by sandwich assays. With an overall time of the assay of 6 hours, the use of sophisticated technologies for the fabrication of the nanowells arrays and for the labeling with enzyme before the detection by fluorescence microscopy, the method does not fulfill the requirements of simplicity, rapidity and possible portability. This calls for maintaining efforts to develop novel solutions.

Using a micrometer-sized particle mobility assay, where particles are tethered to a surface via a DNA fragment with both particles and substrate coated with recognition molecules, Visser et al achieved a continuous monitoring of biomarkers [12] but there is no evidence that the detection related to single-molecules only. Here we push the limits towards a true single-molecule sensing using a single-DNA biochip we have developed to parallelize the analysis of the conformational dynamics of individual DNA molecules by Tethered Particle Motion (TPM) [13] with polystyrene particles of 300 nm diameter. TPM uses videomicroscopy coupled to image analysis to measure the amplitude of motion of nano-sized particles tethered by single DNA molecules to a surface. The amplitude of particle motion is related to the effective length of the DNA tethers and thus reports any change in the conformation of the DNA tether that can be a shortening or an elongation of the molecule but also a looping [14-17], a local bent [18] or a variation in flexibility due to changes in the environment such as the ionic composition [19]. With our single DNA biochip, hundreds of individualized DNA-particle complexes are analysed simultaneously while avoiding interferences between them, improving drastically the resolution, accuracy and response delay of the technique. By a smart coupling of recognition elements to the DNA-particle complexes, we have designed a sandwich assay allowing for the unambiguous detection of the target binding to the pair of recognition molecules (Figure 1). With one recognition molecule grafted to the DNA tether in its middle and the other one coupled to the particles, their bridging mediated by the target induces a looping of the DNA tether revealed by a significative and predictable decrease of the amplitude of particle motion. We chose to use aptamers as recognition molecules because of their easy combination with the DNA-particle complexes used in TPM, in addition to their recognized advantages for biosensors design over antibodies like thermal stability, easy insertion of modifications, reproducible and cost-effective manufacture by chemical synthesis [20]. With a view to obtain a proof-of-concept of an assay applicable/generalizable to target analytes with aptamer pairs, we chose thrombin as target and two aptamers, the 15-mer (HD1) and 29-mer (HD22), selected against thrombin [21, 22], a system considered as a gold standard in the field of aptasensing [23]. Our single-

molecule aptasensing assay detects thrombin in a dose-dependent manner down to concentrations as low as 10 pM with a response delay of 30 minutes without the need for additional reagents.

EXPERIMENTAL SECTION

Chemicals. Thrombin from human plasma (1500-3500 NIH units/mg), bovine serum albumin (BSA), pluronic f-127, neutravidin and carboxylate microspheres (F1-XC-030) were purchased from Sigma-Aldrich. Antidigoxigenin (Fab fragments from sheep) was purchased from Roche Applied Science (Germany). Phosphate buffer (KH_2PO_4 1 mM, Na_2HPO_4 3 mM, NaCl 150 mM, pH 7.4), PBS1X, was prepared from phosphate buffer saline 10X solution (Euromedex, France). PBS1X* corresponds to PBS1X added with 1 mg/mL pluronic f-127 and 0.1 mg/mL BSA. All solutions were prepared using milli-Q purified water.

Aptamers. All oligonucleotides sequences were synthesized by Eurogentec and Eurofins with modifications at the 5'-end position and a 10- or a 20-thymidines spacer for the grafting to the DNA tether or to the particles, respectively. Modifications were either biotin for the binding to neutravidin-coated particles or a sequence of 30 bases (insert) complementary to that remaining in the middle of the DNA tether after enzymatic digestion. Sequences are listed in Table 1.

Name	Sequence
biot-T_{20}-HD1	**5'-biotin-T_{20}-GGTTGGTGTGGTTGG-3'**
insert-T_{10}-HD22	**5'-TCAGCTACAGTAGCCTCAGCTTAGCCATCC-T_{10}-AGTCCGTGGTAGGGCAGGTTGGGGTGACT-3'**
biot-T_{20}-HD22	**5'-biotin-T_{20}-AGTCCGTGGTAGGGCAGGTTGGGGTGACT-3'**
insert-T_{10}-HD1	**5'-TCAGCTACAGTAGCCTCAGCTTAGCCATCC-T_{10}-GGTTGGTGTGGTTGG-3'**
insert-T_{10}- HD22scr	**5'-TCAGCTACAGTAGCCTCAGCTTAGCCATCC-T_{10}-GCGATGCGGATGCGTGAGGTTGCTGAGTG-3'**
HD22c-T_{20}-biot	**5'-AGTCACCCCAACCTGCCCTACCACGGACT-T_{20}-biotin-3'**
HD1c-T_{20}-biot	**5'-CCAACCACACCAACC- T_{20}-biotin-3'**

Table 1: **Oligonucleotide sequences** grafted onto the DNA tether or coupled to the particles.

Preparation of the DNA tether and aptamer grafting. DNA substrates were obtained by PCR amplification from the plasmid template pTOC15 using 5'-biotin forward primer and 5'-digoxygenin reverse primer. Plasmid pTOC15 was derived from plasmid pTOC11, which is itself derived from pBR322 by insertion of 4 out-of-phase A-tracks [18]. A DNA fragment of 59 bp, containing three restriction sites 5'-CCTCAGC-3' for the Nt.BbvCI nicking endonuclease, separated by 15 bp from each other, was inserted between the NheI and BamHI restriction sites of pTOC11.

After purification, the DNA tether was digested by the nickase, the temperature raised to 70°C to dehybridize the 15 b fragments and the 5'-insert-spacer-HD22- 3' oligonucleotide added with a 100-fold molar excess, before decreasing the temperature gradually until room temperature. The grafted DNA tether was further purified before use (see Text S1).

Functionalized DNA/particle complexes formation and htTPM experiments. Neutravidin-coated particles, obtained by chemical crosslinking of neutravidin to the carboxylate particles [13],and HD22-grafted DNA were mixed in PBS1X* at equivalent final molar concentrations of 50 pM each and left at 37°C for 30 min as described in Plénat *et al.* 5'-Biotin-spacer-HD1-3' was added at 10 nM final, and allowed to bind to the particles for an additional 30 min at 37°C.

On the whole, htTPM experiments were carried out as described previously [13]. The htTPM measurements proceed through the videomicroscopy acquisition of images over a field of observation during 1 min at a recording rate of 25 Hz (Figure 1B) using a dark-field microscope (Axiovert 200, Zeiss) equipped with a x32 objective, an additional x1.6 magnification lens and a CMOS camera Falcon 1.4M100 (pixel size 7.4 µm, Dalsa). A dedicated software (Magellium) computes the amplitudes of particles motion over a 2 s sliding interval along the time trace in real time.

The fluidic chambers were made of two glass slides sealed by a 250 µm thick silicone spacer with rectangular cuttings defining fluidic channels of ~10 µL each fed through inlet and outlet holes 1.5 mm in diameter drilled in one of the slides. The other slide is decorated on the internal side with pattern of spots (Figure S1) 800 nm in size, deposited by microcontact printing using poly(dimethylsiloxane) stamps (contact duration of 10 min), previously inked with an antidigoxygenin antibody at 100 µg/mL in PBS.

The channels were first passivated and rinsed using PBS1X*, then 20 µL of the DNA-particle complexes was injected and incubated during 4 hours minimum at room temperature. The channels were further thoroughly rinsed with PBS1X* before starting the measurements in the absence of thrombin and then, eventually, in the presence of thrombin which was added by injection of a volume of 100 µL thrombin solution in PBS1X*.

In the various assays and control experiments, two DNA populations with different conformations and thus amplitudes of motion, looped with A_{looped} = 165 nm and free with A_{free} = 230 nm (the value expected for 2 kb DNA), were expected. The output of the sandwich assay was thus the proportion of looped DNA events in the distributions of the amplitudes of particle motion, referred to as the looped fraction (see Text S1).

For each channel on a biochip, the result is obtained after pooling the amplitudes of motion recorded on three different fields of observation provided that a difference of less than 5% between the proportions of looped DNA over these fields of observation was found, otherwise five fields were accumulated before calculating the looped fraction.

To estimate the reproducibility of the results, acquisitions were repeated with three independent single-DNA biochips for each condition (negative control, a given value of the target concentration, a given ratio of oligonucleotides per particle). Only one condition was tested per channel with images recorded over at least three different fields of observations.

RESULTS AND DISCUSSION

Adaptation of the single-DNA biochip

Design of a sandwich assay using htTPM. The principle of the target detection relies on the monitoring of the expected change in the amplitude of motion of the DNA tethered particles obtained by a smart combination of the pair of recognition molecules to the single DNA biochip (Figure 1). In order to limit non-specific interactions with the surfaces, we chose to graft a single copy of one of the recognition molecules on the DNA tethers while functionalizing the particles with the other recognition molecule at a controled surface density. Upon formation of a sandwich molecular complex, the associated looping of the DNA-particle system is revealed by a decrease of the amplitude of motion to a value defined by the position of the moiety on the DNA tether according to the calibration curve [13].

The amplitude of particle motion A, defined as the square-root of the mean-square displacement calculated over a sliding time interval of 2 s, is monitored in real time by videomicroscopy coupled to image analysis. The single-DNA biochip allows the simultaneous observation of more than 2000 anchoring spots out of which about 500 are occupied by single DNA-particle complexes fully valid for the analysis [13]. Are considered as valid, particles exhibiting a trajectory inscribed in a circle, characterized by a symmetry factor inferior to a threshold value of 1.35, which correspond essentially to those tethered to the surface by a single DNA molecule [13]. Individual traces of the amplitude of particle motion are saved for further scrutiny of the behaviours at the single molecule level. One minute of recording over a microscope field of view is sufficient to compute the distribution of the amplitude of particle motion with good statistics.

In the absence of target, all DNA-particle complexes are in the free state and the distribution of the amplitude of motion exhibits a single population centered on A_{free}. After injection of the target and an incubation period, a second population appears in the distribution around an average value of the amplitude of motion A_{looped} smaller than A_{free} (Figure 1).

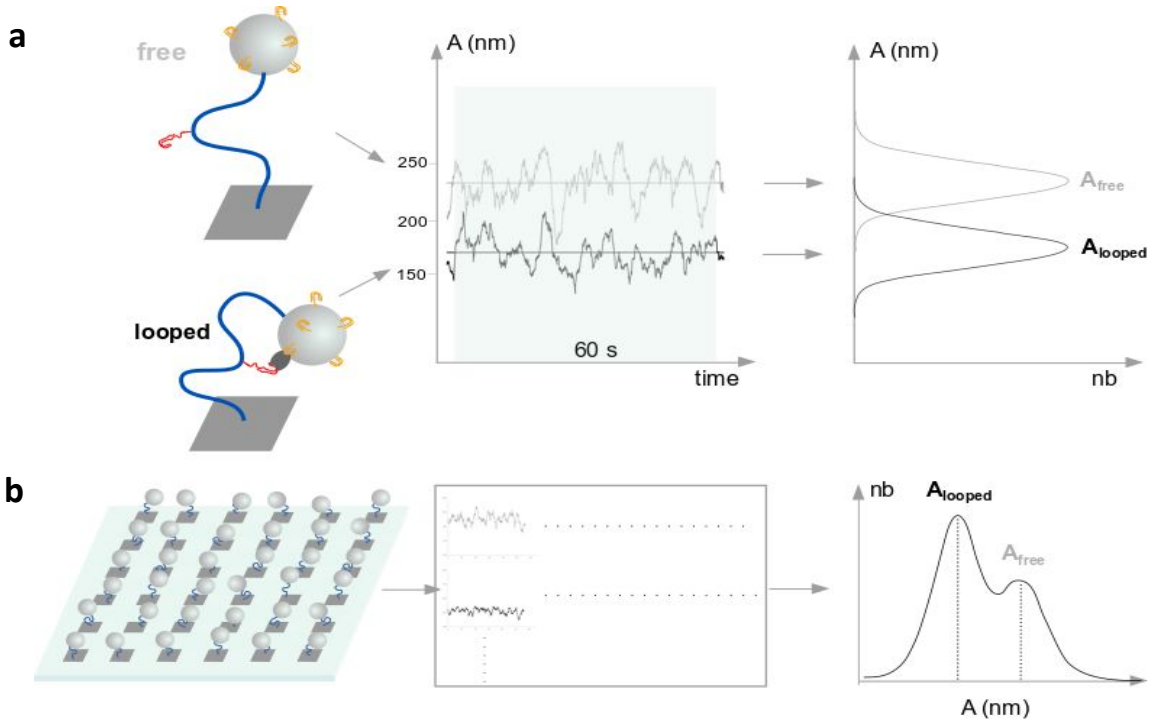

Figure 1: Principles of the detection and the analysis. a In this sandwich assay, a particle functionalized with multiple copies of one aptamer (yellow) is tethered to the surface through a DNA molecule (blue) bearing a single copy of the other aptamer (red). In the absence of the target, the DNA-particle complex is "free" whereas upon binding of the target by both aptamers it is "looped". The monitoring of the amplitude of particle motion by videomicroscopy coupled to image analysis (see Material and Methods) during periods of 60 s allows computing the distribution of the amplitudes of motion. The Gaussian fit of the distribution leads to the determination of the average amplitude of motion which takes two distinct values according to the state of the DNA-particle complex A_{free} or A_{looped} with $A_{looped} < A_{free}$. **b** Using our single-DNA biochip allows to parallelize the analysis and to collect the distribution of the amplitudes of motion of hundreds of DNA-particle complexes in a single acquisition. nb = number of measurements.

Note that this can be due either to a stable looping occurring for a fraction of the DNA-particle complexes upon binding or to a transient looping occurring for a fraction of the DNA-particle complexes that switch between the two states. By fitting the distribution with the sum of two Gaussians we determine the proportion of measures corresponding to a looped state that is the target recognition by the two aptamers. We limit the range of the fit to the data points with A > 100 nm because smaller values result from non-specific and incidental interactions between the DNA tether, particle and surface.

***Integration of aptamers within the single DNA biochip*.** Regarding the DNA tether, the grafted recognition molecule has to be kept at distance from the surface to limit non-specific interactions. The best compromise had to be found to enable a significant decrease of the amplitude of motion upon formation of the sandwich complex in order to have a minimal overlap between the distributions of the free and looped populations. We chose to position the recognition molecule right in the middle of a 2080 bp long DNA molecule. This allows to maximize the difference of amplitude of motion between the free and looped states and to have a looped state with an amplitude of motion clearly distinguishable from that produced by non specific interactions, notably the possible non specific interactions of the particle with the surface. The DNA molecule is functionalized with biotin on one end for binding to the particles and digoxigenin on the other end for anchoring on the spots of the biochip and, contains in its middle, three nickase sites distant by 15 bp for further internal modification as described below (see also Experimental section) (Figure 2).

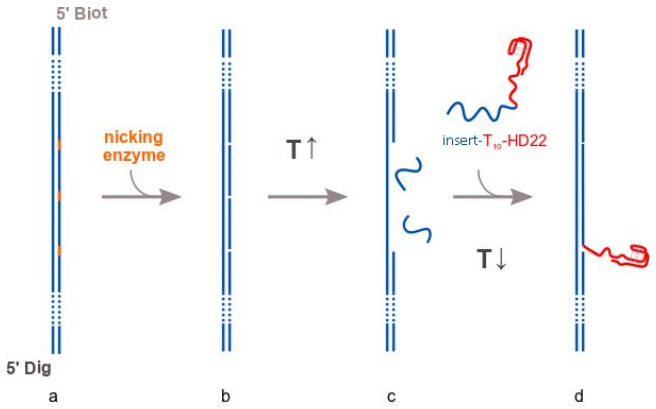

Figure 2: Scheme of the aptamer grafting procedure onto the DNA tether. a The 2 kpb DNA tether contains three restrictions sites (orange) for the Nt.BbvCI nicking endonuclease separated by 15 bp. **b** After cleaving of three distant bases by the enzyme and elevation of the temperature, **c** the two 15 b strands are released. **d** Decreasing the temperature upon addition, in excess, of the aptamer prolonged by a 10 T tract and a sequence complementary to the remaining strand allows the hybridization of the latter and finally the grafting of the aptamer onto the DNA tether.

In order to assess how our assay competes with previously developed approaches, we chose to investigate the well-studied case of the detection of thrombin by the aptamers HD1 and HD22 [12, 24, 25]. These aptamers differ in their ability to bind to thrombin. The G-quadruplex 15-mer aptamer HD1, has the capacity to bind to exosites I and II of the thrombin (with a better affinity for the exosite I) whereas the 29-mer aptamer HD22, mixed structure of G-quadruplex and short duplex, specifically binds to exosite II of thrombin exclusively [21, 22, 26]. HD22 is generally presented as the aptamer having a much better affinity for thrombin than HD1. This stems probably from the K_D determined in their SELEX buffer [21, 22]. Actually wide ranges of K_D values, between about 1 nM and 200 nM, have been reported for both aptamers [25], and references therein, depending on the buffer and the technique. Therefore, we assumed HD22 more affine for thrombin than HD1 and thought that the most favorable configuration would be to graft HD22 in a single copy on the DNA tether and to conjugate HD1 in multiple copies to the particles. The procedures are explained in the next paragraphs.

Regarding the coupling of HD1 to the particles, a spacer has to be introduced to preserve the binding capacity of the aptamer once coupled to the particles surface [27]. We confirmed by Bio-Layer Interferometry measurements (see Text S1 and Figure S2), that addition of a 20-thymidines spacer to the 5' end of the HD1 drastically improves the aptamer binding efficiency. Thus we used oligonucleotides with a biotin modification at the 5' end and a 20-thymidines spacer before the aptamer sequence (biot-T_{20}-HD1 see Table 1) for the strong coupling to carboxylate particles covalently coated with neutravidin, the DNA-particle complex being formed beforehand. Assuming that, below the total coverage of the particles, 100 % of the oligonucleotides would attach to the particles surface, the surface density of HD1 on the particles is simply defined by the HD1/particle ratio at which the incubation is performed.

The grafting of HD22 to the DNA tether proceeds through an internal modification of the DNA. In brief, it consists of dehybridizing two adjacent 15 bases sequences from the DNA molecule and match the remaining 30 bases single stranded sequence by its complementary oligonucleotide, called insert, fused to the aptamer. The detailed procedure depicted in Figure 2 is the following. It starts with the cleaving of three 15 bases distant sites by the nicking endonuclease Nt.BbvcI and the subsequent release of two 15 bases strands by thermal dehybridization at 70°C. The insert fused to a 10 thymidines spacer and the HD22 aptamer, insert-T_{10}-HD22 (see Table 1), is added in large excess with respect to the DNA molecule. The temperature is then slowly decreased till 55°C, an intermediate temperature between the melting temperature of the 30 bp duplex sequence and that of the 15 bp duplex sequences before it is brought to room temperature at which hybridization occurs. Thereafter the 15 bases sequences are eliminated by gel filtration.

The absence of bulk method capable of determining the yield of insertion prompted us to move instead directly to htTPM measurements and evaluate concomitantly the rate of insert grafting and the feasibility of the looping through binding between the particle and the DNA moiety.

For this paramount test, the complementary sequence of HD22, called HD22c, was coupled to the particles in place of HD1. As a preliminary control, we compared the amplitudes of motion measured for particles coated with neutravidin only and with bare and modified DNA tethers. Each condition showed a single population with equal average amplitude of motion of 230 nm corresponding to A_{free} within the experimental error (Table S1). When the biot-T_{20}-HD22c was coupled to the particles and the DNA tether grafted with HD22, a second population of DNA-particle complexes was observed the proportion of which increased with increments of the HD22c/particle ratio (Figure 3).

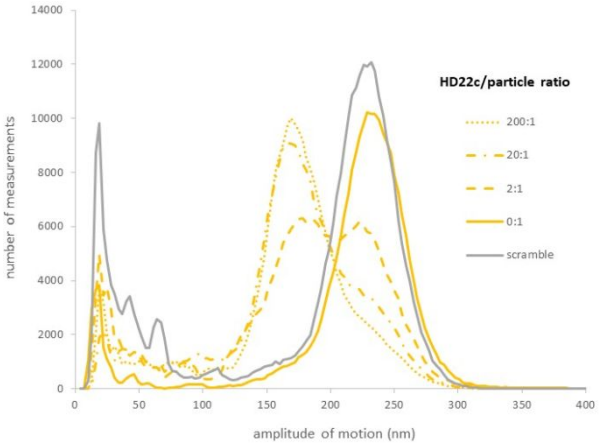

Figure 3: Distribution of the amplitudes of motion of the particles with HD22 grafted to the DNA tether and HD22c coupled to the particles as a function of the HD22c per particle ratio. A looped population is observed, increasing with the density of HD22c at the surface of the particles, which is not detected with neutravidin-only particles or if scrambled HD22 is grafted onto the DNA tether.

This second population was not detected for DNA grafted with scrambled-HD22 using insert-T_{10}- HD22scr (see Table S1), nor with neutravidin-only particles as already mentioned. As deduced from the double Gaussian fit of the total distribution, the average amplitude of motion of this population is equal to 165 ± 2 nm (A_{looped}^{max} ± SEM) corresponding to the expected value for the looped state of the DNA-particle complex, A_{looped}. The fraction of looped state reached 91% for an HD22c/particle ratio of 200/1 corresponding to an « occupied » fraction of the particles surface of approximately 10 % (Text S2). This result is quite satisfactory and allowed us to consider our DNA modification protocol as valid as well as the detection assay through the observation of a looped state as feasible.

Detection of thrombin

The formation of a sandwich complex is detected. Before embarking in the detection assays of thrombin by htTPM, we verified by BioLayer Interferometry that both HD1 and HD22 aptamers keep their binding capacity to thrombin in the standard buffer used in htTPM experiments, PBS1X*, composed of PBS1X added with two blocking agents Pluronic F-127 and BSA (see Figure S3). In addition, to ensure that the optimal conditions were met for a quantitative detection of thrombin by htTPM, we had to check that the binding of thrombin to only one of the aptamer do not lead to a significative decrease of the amplitude of motion and to determine the aptamer to particle ratio that maximizes the looped fraction of DNA-particle complexes. To do so, we acquired a series of measurements after a 30 min incubation of thrombin solutions in PBS1X* following the preparation of the single DNA biochip for the htTPM measurements. This time interval was chosen in order to ensure that the measurements were performed at equilibrium.

Firstly, compared to the amplitude of motion measured for the bare DNA tether alone, no change of the amplitude of motion was observed, except for uncertainty, at a relatively high concentration of thrombin equal to 1 nM, when no or only one aptamer was installed on the biochip, either HD22 grafted to the DNA tether or HD1 bound to the particles (Figure S4).

Secondly, we compared the fractions of looped states obtained at a low concentration of thrombin of 10 pM for various HD1 aptamer to particle ratios in the range 2:1 to 2000:1. Considering the radii of the particles of 150 nm and the typical size of a neutravidin molecule of 5 nm, respectively, the particles harbour a maximum of about 10^4 neutravidin molecules at their surface. Assuming that only half of their binding sites, four in number, are accessible to biotin conjugated aptamers, this leaves 2 10^4 sites available. We hypothesized that seeking for a full occupation of the neutravidin binding sites would require a large excess of HD1 to overcome excluded volume interactions raising the question of its total elimination and we did not exceed an aptamer to particle ratio corresponding to 10% of the available sites. It proved to be reasonable since a significant and maximal fraction of looped states was obtained for an aptamer to particle ratio of 200:1 (Figure S5). We chose to use this condition to examine further whether the signal varied with the thrombin concentration.

The same experimental procedure was used with the measurements acquisition performed 30 min after the injection of the thrombin solution in the fluidic channel. The reported fractions of looped states have

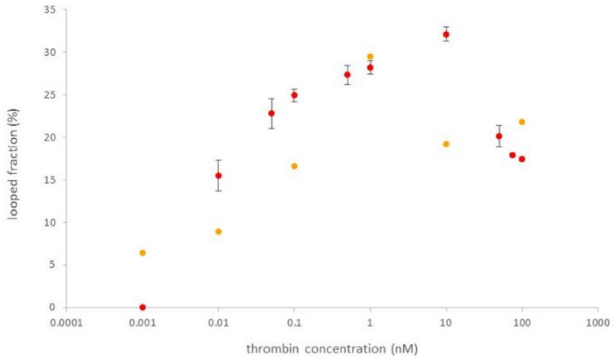

been calculated from measurements over at least three different fields of observation per channel cumulating more than 1000 valid particles, and in triplicate for each concentration tested (Figure 4). No increments of the concentration were applied, only one concentration of thrombin was analyzed per channel. The looped fraction versus thrombin concentration curve increases monotonically between 1 pM and 10 nM at which it reaches a maximum of 33 % before droping rapidly by half.

Figure 4: Dose-response curves for the single-molecule sandwich aptasensing assay. The variation of the looped fraction of the DNA-particle complexes as a function of thrombin concentration is reported for two configurations of the assay with either insert-T_{10}-HD22 grafted onto the DNA tethers and HD1 coupled to the particles (red) or, insert-T_{10}-HD1 grafted onto the DNA tethers and HD22 coupled to the particles (orange). In this latter case, the data points are re-scaled for the difference in the looped fraction found with the complementary oligonucleotides bound to the particles (see Table S2 for raw data).

To check if the chosen configuration for the sandwich assay was the best, i.e. HD22 on the DNA tether and HD1 on the particle, we tested the inverse option that is HD22 coupled to the particles and HD1 grafted on the DNA tether. The results of similar series of measurements are reported in Figure 4. Note that in this latter case, the largest looped fraction attainable which was estimated by coupling the oligonucleotide complementary to HD1 to the particles was found about 20% lower than the precedent one. Nevertheless, the overall shape of the dose-response curve for this inverted configuration is similar with a drop after a maximal value of the looped fraction at 1 nM thrombin concentration. For better comparison, the fractions of looped state reported in Figure 4 have been rescaled relative to the maximum attainable for each configuration of the assay (see raw data in Table S2). The assay with HD22 grafted on the DNA tether shows larger dynamic and analytic ranges.

***The limit of detection (LOD) is in the picomolar range*.** Based on the most pessimistic estimate for the significance threshold of the looped fraction, which we set to 5%, the LOD is found around 10 pM for both configurations. In particular with the assay where HD22 was grafted on DNA, a looped fraction of 15 % is

measured, a value equal to three times the significance threshold. Above this limit, a dose-dependent response is observed with an increase of the looped fraction with the thrombin concentration to a value of about 30% and then drops down to about 20%.

A simple reasoning can account for the low value of the LOD. It starts with the fact that the probability of binding of a thrombin molecule to a particle via one of the aptamers coupled to it is higher than that of its binding to the aptamer grafted to the DNA tether. Then, it must be considered that once a molecule of thrombin is captured by a particle, the local thrombin concentration experienced by the aptamer grafted to the DNA tether is very high and promotes the binding of thrombin leading to the sandwich complex. The local concentration of thrombin reads:

$$C_{local} = \frac{1}{V_{local}} = \frac{1}{\frac{2}{3}\pi R^3 N_A}\,(M)$$

where R (in 10^{-1}m) is the radius of the half sphere occupied by the tethered particle around its anchoring point and N_A the Avogadro number. Approximating R by the average amplitude of motion in the free state, R ~ A_{free} with A_{free} = 230 nm, gives C_{local} = 65 nM. The fraction of particles that would then be involved in a sandwich complex, f_{folded}, can be estimated from the following equation derived from the law of mass action :

$$f_{folded} = \frac{C_{local}}{C_{local} + K_D}$$

Assuming K_D = 2 nM, a value comprised between 1.2 and 3.2 nM found for HD1 and HD22, respectively, in PBS, the same buffer as that used in the present study [24], this gives f_{folded} = 97 %. The limiting factor is thus the fraction of particles, which have bound a thrombin molecule, $f_{bound\,part}$, that can be evaluated using the following equation:

$$f_{bound\,part} = 200\,\frac{C}{C + K_D}$$

adapted from the Langmuir isotherm equation to take into account the aptamer to particle ratio and where C is the « bulk » thrombin concentration. Assuming again the same value of 2 nM for K_D, a value of 15% of the fraction of bound particles with one thrombin in average would be obtained for a thrombin concentration equal to 1.5 pM. This theoretical prediction for the LOD value stands for ideal conditions and must be revised upwards to account for unavoidable experimental pitfalls such as the rate of accessible aptamers coupled to the particles and the statistical variability of the number of thrombin bound per particle. Therefore, we conclude to a good agreement, within one order range, between the estimated and experimentally determined LOD and, at the same time, to the validity of the approximate values of both K_D (2 nM) chosen for our calculations, in this context.

Nevertheless, the two configurations could lead to a somewhat distinct LOD due to differences in the exact K_D values for each aptamer and the ability of HD1 to bind also to the exosite II targeted by HD22 aptamer with an expected lower affinity however.

***The analytic range extends over three decades of target concentration*.** Above the LOD, a dose-dependent response is observed with an increase of the looped fraction with the thrombin concentration from 10 pM to 10 nM at which it reaches a value of about 30% and then drops down about half.

Obviously the maximum of looped fraction is attained when all aptamers are either bound to a thrombin or inaccessible due to a volume exclusion effect and the formation of the sandwich complex then impeded. In one-step immunoassays such a situation occurs at high analyte concentration and gives rise to the so-called « hook » effect [28]. In our assay, we would expect this « hook » effect to take place at a concentration of thrombin much larger than the K_D to have not only all accessible aptamers on the particles but also all single aptamers grafted to the DNA tethers bound to thrombin. However, the peak is observed around 10 nM only, a concentration at which hardly more of half of these sites would be expected to be occupied and thus below the conditions for a Hook effect. A finding reported by Daniel et al [25] and confirming a first observation by Tang et al in 2007 [27] sheds an interesting light that might explain our observation. Monitoring the formation of sandwich complexes using Surface Plasmon Resonance they observed an acceleration of the dissociation rate of the thrombin bound to spots of « capture » aptamers after injection

of the « reporter » aptamer. This suggests that thrombin, at least when bound at relatively high density to surface coupled aptamers, is displaced by free aptamers in solution. Thereby, in our assay, the aptamers grafted to the DNA tethers might behave as free aptamers and catch thrombin molecules bound to their neighboring particles when their coverage density exceeds a certain value. At the same time this could explain that the maximal fraction of looped state found is rather moderate.
Overall, the possible interference due to a dissociation of thrombin bound to particles coupled aptamers by the aptamer grafted to the DNA tethers would deserve further testing in the future because a better understanding of the mechanisms at play in this assay would allow to find conditions for even better performances.

***Stability of the sandwich complexes*.** So far, we have discussed a global analysis of the amplitudes of motion measurements pooling together all the data acquired over hundreds of particles to build the distributions of amplitude of motion and determine the respective of fractions of free and looped populations.

Proceeding this way proves to be efficient in producing a reliable detection and quantification of the concentration of thrombin but masks the behaviours of single sandwich HD1-thrombin-HD22 complexes. However, the htTPM technique allows accessing the individual time traces and we scrutinized those to examine whether the looped states were stable or if switching events between the two states occurred. As illustrated in Figure 5 were we reported two typical time traces, A = f(t) measured during the 1 min duration of a measurement, the amplitude of motion of a given DNA-particle complex analyzed 30 min after thrombin injection remained either free or looped.

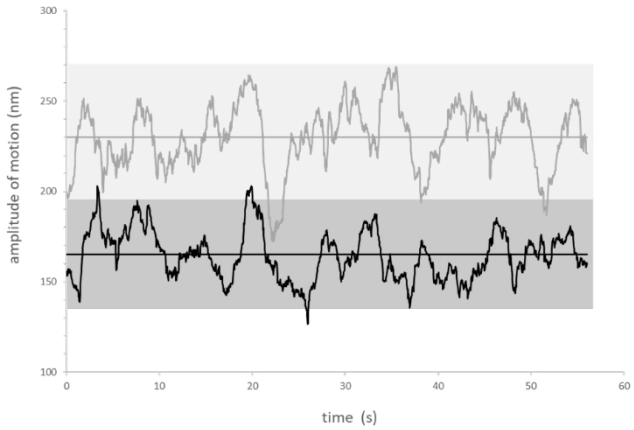

Figure 5: Temporal stability of the sandwich complexes. Typical time traces of the amplitude of motion of DNA-particle complexes recorded 30 min after injection of thrombin. The traces fluctuate within intervals of 2 x SD around the average amplitudes of motion of 230 nm (grey) for the free state or 165 nm (black) for the looped state.

Indeed, the traces fluctuate within an interval of 2 x SD around a constant average amplitude of motion of either 230 nm or 165 nm. Scanning recordings acquired at 100 pM and 10 nM thrombin with HD22 on the DNA tether, we could find only 3% of DNA-particle complexes exhibiting a single transition, predominantly an unlooping, and 4 % experiencing some switching events between free and looped states. Based on these observations at the single molecule level, we can conclude that once a sandwich complex is formed it has a lifetime of more than 60 s. This result is consistent with the ensemble measurements by SPR of the residence times of about 250 s for HD1 in exosite I and HD22 in exosite II [24]. In contrast, it is at odd with the lifetime of 9 s found for the bound states in the particle mobility assay of Visser et al [12] but the difference in the geometry of their assay can explain this apparent discrepancy. The DNA tether measuring there only 40 nm, which is shorter than the dsDNA persistence length, is more likely to behave as a rigid rod[19, 29]. The excluded-volume effect due to the proximity of the particle from the surface results in an entropy-driven stretching force acting on the DNA molecule, which is all the greater, as the ratio of the particle size over the DNA size is the larger[30, 31]. This force pulling the particle apart from the surface affects the binding kinetics, resulting in a short lifetime of the sandwich complex.

Overall, our experimental results demonstrate the successful development of a single-molecule sandwich assay based on the combination of our single-DNA biochip with aptamers. The method proves to have remarkable properties for the detection and quantification of molecular targets: low LOD in the picomolar

range, short response time within a delay of 30 minutes, ease of use with only one-step procedure namely the sample injection and no need for additional reagent.

CONCLUSION

The development of aptamer sensors for thrombin has attracted continuous interest since 15 years. Strikingly, the most recently designed platforms for the detection of the formation of an aptamer-thrombin-aptamer sandwich make use of nano- or micro-particles in a variety of techniques. Au nanoparticles allow to enhance SPR signal and reach a limit of detection of 100 pM [32]. In this assay, the formation of the sandwich proceeds in two steps. Thrombin is captured by the aptamer immobilized on the surface and then detected through the binding of the other aptamer conjugated to Au nanoparticles. This disadvantage is counterbalanced by the possibility to regenerate the sensing surface. A similar process is at work in a sensitive electrochemical sensor based on Au-metal oxide nanoparticles conjugated to the detection aptamer but involving also the decoration of the electrode surface with Ag nanowires [33]. Here the extremely low detection limit of 0.5 pM is at the expense of the ease of implementation and the possibility to re-use the aptasensor. Magnetic beads conjugated to a capture aptamer offer the advantage of facilitating the separation of the target from the solution. The supension array technology, which exploits such micrometer-sized beads, proved to have a poor sensitivity with a limit of detection of 0.5 nM [34]. Better performances were obtained in an aggregation assay using smaller magnetic particles monitored by resonance light scattering [35]. The method provides a linear response over two decades of concentrations in the range 60 pM to 6 nM and the aptamer-conjugated particles are re-usable by a simple heating at 50°C that is supposed to induce the unfolding of the G quadruplex structures of both aptamers and thus the release of thrombin. Finally, in the “cousin” particle mobility assay of Visser et al, the LOD falls around 10 nM[12].

In conclusion, our single-molecule sandwich aptasensing approach is efficient and well-positionned with regard to the state-of-the-art. Transposable to antibodies as recognition molecules, our technique has also advantages over the standard sandwich ELISA owing to the short response time and simplicity of use. In addition, htTPM has potential for multiplexed detection and miniaturization. Distinct DNA-particle complexes can be designed and mixed to detect different molecules simultaneously. For example, different particle sizes could be used to identify the DNA-particle complexes combined to a given pair of aptamers through a specific dark-field imaging signature. Finally, thanks to the simplicity of the principle of detection and of the imaging mode, extreme miniaturization such as smartphone-based devices can be envisaged [36].

AUTHOR INFORMATION

e-mails : diasoukarie@gmail.com (Diana Soukarié), rousseau@ibcg.biotoul.fr (Philippe Rousseau), maya.salhi-hernandez@inrae.fr (Maya Salhi), alexia.de-caro@ipbs.fr (Alexia de Caro), escudier@chimie.ups-tlse.fr (Jean-Marc Escudier), catherine.tardin@ipbs.fr (Catherine Tardin), vincent.ecochard@ipbs.fr (Vincent Ecochard)

ACKNOWLEDGMENTS

D.S. thanks the Agence Innovation Défense and Université Paul Sabatier for PhD funding. The authors thank Caroline Ladurantie, Serge Mazères and Lionel Mourey for technical support and GTP Technology for the loan of the BLItz™ apparatus.

COMPETING INTERESTS STATEMENT

Authors have no competing interests to declare.

SUPPORTING INFORMATION

Experimental complements. Estimate of particle’s coverage. Assembly of htTPM fluidic chamber. Interactions of thrombin with HD22 and HD1 aptamers (BLI sensorgrams). Distribution and values of the amplitude of motion in various conditions. Looped fraction with HD22 and HD1 grafted DNA for various thrombin concentrations.

REFERENCES

1. Ahmed, M. U.; Saaem, I.; Wu, P. C.; Brown, A. S., Personalized diagnostics and biosensors: a review of the biology and technology needed for personalized medicine. *Critical Reviews in Biotechnology* **2014,** *34* (2), 180-196.
2. Sousa, J. C. G.; Ribeiro, A. R.; Barbosa, M. O.; Pereira, M. F. R.; Silva, A. M. T., A review on environmental monitoring of water organic pollutants identified by EU guidelines. *Journal of Hazardous Materials* **2018,** *344*, 146-162.
3. Luo, Y.; Guo, W.; Ngo, H. H.; Nghiem, L. D.; Hai, F. I.; Zhang, J.; Liang, S.; Wang, X. C., A review on the occurrence of micropollutants in the aquatic environment and their fate and removal during wastewater treatment. *Science of The Total Environment* **2014,** *473-474*, 619-641.
4. Kim, J.; Campbell, A. S.; de Ávila, B. E.-F.; Wang, J., Wearable biosensors for healthcare monitoring. *Nature Biotechnology* **2019,** *37* (4), 389-406.
5. Dincer, C.; Bruch, R.; Kling, A.; Dittrich, P. S.; Urban, G. A., Multiplexed Point-of-Care Testing – xPOCT. *Trends in Biotechnology* **2017,** *35* (8), 728-742.
6. Soukarié, D.; Ecochard, V.; Salomé, L., DNA-based nanobiosensors for monitoring of water quality. *International Journal of Hygiene and Environmental Health* **2020,** *226*, 113485.
7. Farka, Z.; Juřík, T.; Kovář, D.; Trnková, L.; Skládal, P., Nanoparticle-Based Immunochemical Biosensors and Assays: Recent Advances and Challenges. *Chemical Reviews* **2017,** *117* (15), 9973-10042.
8. Wu, Y.; Tilley, R. D.; Gooding, J. J., Challenges and Solutions in Developing Ultrasensitive Biosensors. *Journal of the American Chemical Society* **2019,** *141* (3), 1162-1170.
9. Liu, H.; Lei, Y., A critical review: Recent advances in “digital” biomolecule detection with single copy sensitivity. *Biosensors and Bioelectronics* **2021,** *177*, 112901.
10. Gooding, J. J.; Gaus, K., Single-Molecule Sensors: Challenges and Opportunities for Quantitative Analysis. *Angewandte Chemie International Edition* **2016,** *55* (38), 11354-11366.
11. Rissin, D. M.; Kan, C. W.; Campbell, T. G.; Howes, S. C.; Fournier, D. R.; Song, L.; Piech, T.; Patel, P. P.; Chang, L.; Rivnak, A. J., Single-molecule enzyme-linked immunosorbent assay detects serum proteins at subfemtomolar concentrations. *Nature Biotechnology* **2010,** *28* (6), 595-599.
12. Visser, E. W. A.; Yan, J. H.; van IJzendoorn, L. J.; Prins, M. W. J., Continuous biomarker monitoring by particle mobility sensing with single molecule resolution. *Nat Commun* **2018,** *9*.
13. Plenat, T.; Tardin, C.; Rousseau, P.; Salome, L., High-throughput single-molecule analysis of DNA-protein interactions by tethered particle motion. *Nucleic Acids Res* **2012,** *40* (12), e89.
14. Pouget, N.; Turlan, C.; Destainville, N.; Salome, L.; Chandler, M., IS911 transpososome assembly as analysed by tethered particle motion. *Nucleic Acids Res* **2006,** *34* (16), 4313-23.
15. Diagne, C. T.; Salhi, M.; Crozat, E.; Salomé, L.; Cornet, F.; Rousseau, P.; Tardin, C., TPM analyses reveal that FtsK contributes both to the assembly and the activation of the XerCD-dif recombination synapse. *Nucleic Acids Res* **2014,** *42* (3), 1721-1732.
16. Zurla, C.; Manzo, C.; Dunlap, D.; Lewis, D. E. A.; Adhya, S.; Finzi, L., Direct demonstration and quantification of long-range DNA looping by the λ bacteriophage repressor. *Nucleic Acids Res* **2009,** *37* (9), 2789-2795.
17. Johnson, S.; van de Meent, J.-W.; Phillips, R.; Wiggins, C. H.; Lindén, M., Multiple LacI-mediated loops revealed by Bayesian statistics and tethered particle motion. *Nucleic Acids Res* **2014,** *42* (16), 10265-10277.
18. Brunet, A.; Chevalier, S.; Destainville, N.; Manghi, M.; Rousseau, P.; Salhi, M.; Salome, L.; Tardin, C., Probing a label-free local bend in DNA by single molecule tethered particle motion. *Nucleic Acids Res* **2015,** *43* (11), e72.
19. Guilbaud, S.; Salome, L.; Destainville, N.; Manghi, M.; Tardin, C., Dependence of DNA Persistence Length on Ionic Strength and Ion Type. *Phys Rev Lett* **2019,** *122* (2), 028102.
20. Mascini, M., *Aptamers in bioanalysis*. John Wiley & Sons: 2009.
21. Bock, L. C.; Griffin, L. C.; Latham, J. A.; Vermaas, E. H.; Toole, J. J., Selection of single-stranded DNA molecules that bind and inhibit human thrombin. *Nature* **1992,** *355* (6360), 564-6.
22. Tasset, D. M.; Kubik, M. F.; Steiner, W., Oligonucleotide inhibitors of human thrombin that bind distinct epitopes. *J Mol Biol* **1997,** *272* (5), 688-98.

23. Deng, B.; Lin, Y.; Wang, C.; Li, F.; Wang, Z.; Zhang, H.; Li, X.-F.; Le, X. C., Aptamer binding assays for proteins: The thrombin example—A review. *Analytica Chimica Acta* **2014,** *837*, 1-15.
24. Trapaidze, A.; Herault, J. P.; Herbert, J. M.; Bancaud, A.; Gue, A. M., Investigation of the selectivity of thrombin-binding aptamers for thrombin titration in murine plasma. *Biosens Bioelectron* **2016,** *78*, 58-66.
25. Daniel, C.; Melaine, F.; Roupioz, Y.; Livache, T.; Buhot, A., Real time monitoring of thrombin interactions with its aptamers: insights into the sandwich complex formation. *Biosens Bioelectron* **2013,** *40* (1), 186-92.
26. Pica, A.; Russo Krauss, I.; Parente, V.; Tateishi-Karimata, H.; Nagatoishi, S.; Tsumoto, K.; Sugimoto, N.; Sica, F., Through-bond effects in the ternary complexes of thrombin sandwiched by two DNA aptamers. *Nucleic Acids Res* **2017,** *45* (1), 461-469.
27. Tang, Q.; Su, X.; Loh, K. P., Surface plasmon resonance spectroscopy study of interfacial binding of thrombin to antithrombin DNA aptamers. *Journal of Colloid and Interface Science* **2007,** *315* (1), 99-106.
28. Schiettecatte, J.; Anckaert, E.; Smitz, J., Interferences in immunoassays. *Advances in immunoassay technology* **2012,** *3*, 45-62.
29. Panja, D.; Barkema, G. T.; van Leeuwen, J. M. J., Dynamics of a double-stranded DNA segment in a shear flow. *Physical Review E* **2016,** *93* (4), 042501.
30. Kumar, S.; Manzo, C.; Zurla, C.; Ucuncuoglu, S.; Finzi, L.; Dunlap, D., Enhanced tethered-particle motion analysis reveals viscous effects. *Biophys J* **2014,** *106* (2), 399-409.
31. Segall, D. E.; Nelson, P. C.; Phillips, R., Volume-exclusion effects in tethered-particle experiments: bead size matters. *Phys Rev Lett* **2006,** *96* (8), 088306.
32. Bai, Y.; Feng, F.; Zhao, L.; Wang, C.; Wang, H.; Tian, M.; Qin, J.; Duan, Y.; He, X., Aptamer/thrombin/aptamer-AuNPs sandwich enhanced surface plasmon resonance sensor for the detection of subnanomolar thrombin. *Biosensors and Bioelectronics* **2013,** *47*, 265-270.
33. Zhang, Q.; Fan, G.; Chen, W.; Liu, Q.; Zhang, X., Electrochemical sandwich-type thrombin aptasensor based on dual signal amplification strategy of silver nanowires and hollow Au-CeO2. *Biosens Bioelectron* **2020,** *150*, 111846.
34. Liu, Y.; Liu, N.; Ma, X.; Li, X.; Ma, J.; Li, Y.; Zhou, Z.; Gao, Z., Highly specific detection of thrombin using an aptamer-based suspension array and the interaction analysis via microscale thermophoresis. *Analyst* **2015,** *140* (8), 2762-70.
35. Hou, Y.; Liu, J.; Hong, M.; Li, X.; Ma, Y.; Yue, Q.; Li, C.-Z., A reusable aptasensor of thrombin based on DNA machine employing resonance light scattering technique. *Biosensors and Bioelectronics* **2017,** *92*, 259-265.
36. Huang, X.; Xu, D.; Chen, J.; Liu, J.; Li, Y.; Song, J.; Ma, X.; Guo, J., Smartphone-based analytical biosensors. *Analyst* **2018,** *143* (22), 5339-5351.

For Table of Contents Only